Molecular Crystals and Liquid Crystals
Publication details, including instructions for authors and subscription information:
http://www.tandfonline.com/loi/gmcl16

The Distribution of Thickness Irregularities Shows Myelin is Paracrystalline

Albert Hybl [a]

[a] Department of Biophysics, University of Maryland School of Medicine, Baltimore, Maryland, 21201

Version of record first published: 21 Mar 2007.

To cite this article: Albert Hybl (1976): The Distribution of Thickness Irregularities Shows Myelin is Paracrystalline, Molecular Crystals and Liquid Crystals, 36:3-4, 271-278

To link to this article: http://dx.doi.org/10.1080/15421407608084331

Mol. Cryst. Liq. Cryst., 1976, Vol. 36, pp. 271–278

Printed in Holland

The Distribution of Thickness Irregularities Shows Myelin is Paracrystalline

ALBERT HYBL

Department of Biophysics, University of Maryland School of Medicine, Baltimore, Maryland 21201

(*Received October 6, 1975; in final form July 28, 1976*)

Measurements of thickness irregularities from an electron microscopic cross section of myelin sheath shows that the myelin lamellar structure is paracrystalline. Reinterpretation of the myelin X-ray diffraction data is consistent with a paracrystalline model.

I INTRODUCTION

A Historical

The discovery by Schmitt, Bear and Clark[1] that myelin scatters X-rays indicated a structural periodicity. Electron microscopy studies by Geren[2] showed that the myelin sheath is formed from a spirally wrapped cell membrane. The lamellar structure of native frog sciatic nerve myelin has a one dimensional periodicity, d, measured by X-ray diffraction of 170 Å and gives up to sixteen low order X-ray reflections. The intensities of these reflections contain information about the average electron density distribution projected upon a radial line. Innumerable attempts have been made to unlock this information.[3–9] In all of these studies the myelin lamellar stacking was implicitly assumed to be crystalline. The possibility that the spiral wrapping mechanism would or could produce a paracrystalline structure appears to have been overlooked.

The lamellar layers in myelin are formed by successive wrapping of a Schwann cell about an axon membrane. The outer membrane surfaces from two contiguous wrappings of the Schwann cell come together to form an exoplasmic aqueous-protein band. The inside membrane surfaces of each

Schwann cell wrapping come in apposition to form a cytoplasmic aqueous-protein band. Between two exoplasmic bands and one central cytoplasmic band are two bands of bimolecular lipids. Because myelin is formed from enfolding of a single Schwann cell, the lipid bands are equivalent; that is, they are related by a mirror plane located at the center of the cytoplasmic protein band. Two contiguous wrappings of the Schwann cell are likewise related by a mirror plane located at the midpoint of the exoplasmic protein band. Owing to the component heterogeneity, these mirror planes represent only a local statistical symmetry relation between adjacent layers of Schwann cell membrane. (Detailed molecular asymmetries are neglected in this description.)

The constituents that give myelin its primary structure are the lipids. They account for approximately 80% of the mass of myelin. A diversity of lipids is found belonging to a variety of classes including phosphatidyl-ethanolamine, phosphatidycholine, glycolipids, sphingomyelin, cholesterol, etc. The long hydrocarbon chains appear in many different lengths and several degrees of unsaturation. Proteins comprise another important class of constituents, accounting for 20% of the membrane mass. An aqueous environment surrounds these proteins. As with the lipids, a variety of proteins are found.

B Two models for the lamellar stacking in myelin

The parallel contiguous repetitions of identical membrane lamellae give rise to the crystalline stacking model. The lamellar repeat period is constant. Compositional variations in the lipids and proteins must be compensated by local adjustments in the distribution of water. In the crystal stacking model, myelin can be considered the convolution of two functions—one representing the projected radial electron density and the other a sharp one-dimensional lattice peak function with periodic spacing d. Local disorder gives rise to a normal distribution of small displacements about each lattice point. Hosemann and Bagchi[10] have called these displacements "distortions of the first kind." After m spiral wrappings the thickness, T_m, for myelin would be md. The standard deviation of T_m, S_m, is invariant with respect to the number of wrappings; that is, for all values of m, the standard deviation of T_m would be a constant ($S_m = s$).

In the paracrystalline[10] model the lamellar thicknesses, labelled $d_1, d_2, \ldots, d_m$, vary greatly owing to component heterogeneity, variation in water content, and variations in molecular configuration and/or molecular tilt. After m spiral wrappings the myelin thickness would be $T_m = d_1 + d_2 + \cdots + d_m$. Since the d_j are independent measurements of a single specimen membrane with mean lamellar thickness d and standard deviation s, the

measurements of T_m at various random locations along or around the axon will be normally distributed with mean $\bar{T}_m = md$ and standard deviation $S_m = s\sqrt{m}$. The stacking irregularities in this case are known as "distortions of the second kind."

The distinction between the crystalline stacking model and the paracrystalline model is made from measurements of the lamellar spacing variances for increasing values of m. Small variations that are invarient with respect to the number of wrappings would prove the stacking to be crystalline. If on the other hand, the standard deviation of T_m contains the factor $\sqrt{m}$, the stacking model must be paracrystalline. An electron microscopic cross section through a specimen of myelin sheath was available and was used to partially resolve the problem.

II RESULTS FROM ELECTRON MICROSCOPY MEASUREMENTS

Figure 1 shows a cross section through a portion of myelin sheath from a cat peripheral autonomic nerve. Values of T_m were measured normal to the lamellae at various circumferential intervals around the sheath. Table I lists values of m, $\bar{d}_m$, $\bar{T}_m$, S_m, and $S_m/\sqrt{m}$. These results show that for fixed,

TABLE I

Tabulation of the standard deviation of myelin thickness for various values of m

m	$\bar{d}_m$ (Å)	$\bar{T}_m$ (Å)	S_m (Å)	$S_m/\sqrt{m}$ (Å)
1	131	131	7.2	7.2
2	129	260	5.7	4.1
3	122	382	8.5	4.9
4	123	505	13.2	6.6
5	126	631	10.6	4.7
6	125	756	16.1	6.6
7	125	881	19.6	7.4
8	126	1007	20.5	7.2
9	125	1132	22.1	7.4
10	125	1257	24.7	7.8
11	128	1385	26.0	7.8
12	125	1510	23.8	6.9
13	128	1638	24.6	6.8
14	130	1768	22.8	6.1
15	127	1895	30.8	8.0

Values of the standard deviation were computed from measurements of T_m at 8 circumferential positions in the cat peripheral nerve myelin sheath shown in Figure 1. $\bar{T}_m = (T_{1m} + T_{2m} + \cdots + T_{8m})/8$; $\bar{d}_m = \bar{T}_m - \bar{T}_{m-1}$.

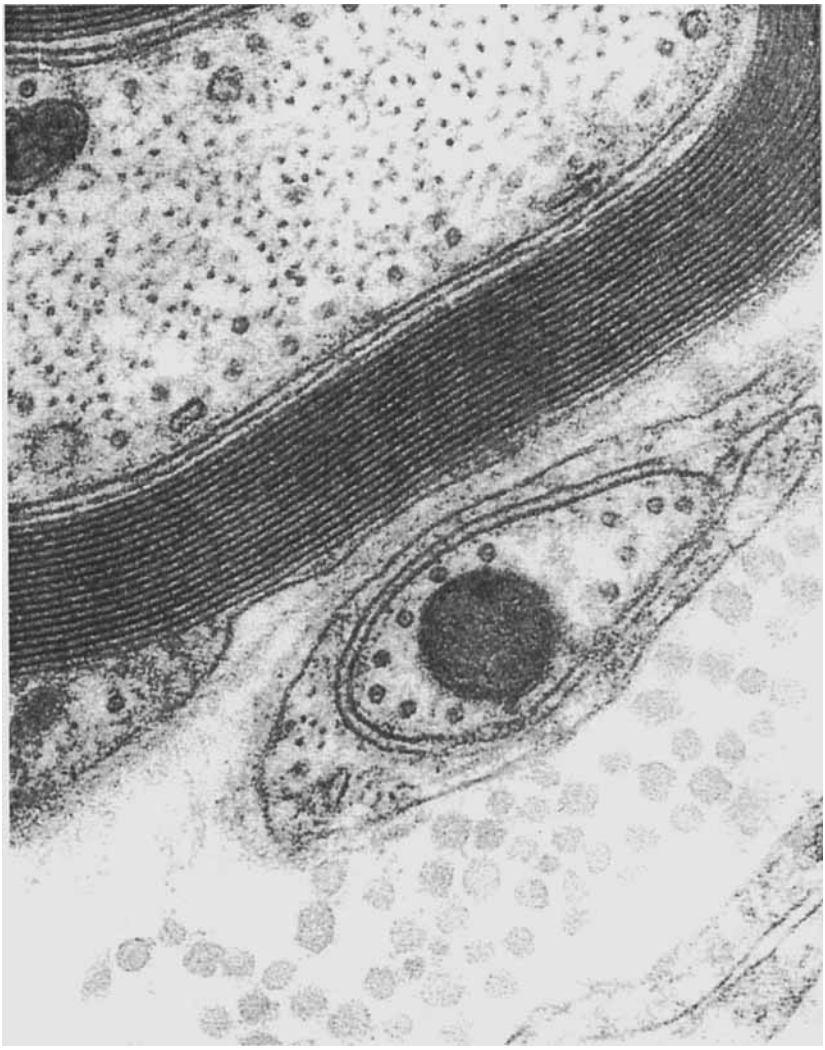

FIGURE 1 An electron micrograph showing part of a myelin sheath from a cat autonomic peripheral nerve double fixed with glutaraldehyde and osmium tetroxide, embedded in Epon followed by section staining with lead citrate and uranyl acetate. (Magnification: 87,000×). Photograph kindly supplied by Dr. Marshall L. Rennels.

embedded, stained and sectioned myelin the standard deviation in lamellar thickness contains the factor $\sqrt{m}$ and that the paracrystalline stacking model is the correct representation for the propagation of stacking irregularities. It also shows that s ranges roughly between 4–8 Å with a mean value of 6.6 Å.

A normalized distribution function[11] of spacings between layers d_1 and d_m has the form:

$$H_m(x + md) = \frac{1}{s\sqrt{2\pi m}} \exp\{-\tfrac{1}{2}(x^2/s^2 m)\}; \int_{-\infty}^{\infty} H_m(x + md)dx = 1$$

$H_m(x + md)$ is a distribution function that exhibits an increasing deterioration of lamellar regularity with increasing m.

Do measurements by electron microscopy of myelin tissue which has been fixed, embedded, stained and sectioned represent the true structure of native hydrated myelin? Has the tissue preparative procedure prior to the electron micrographic examination resulted in a transition from the crystalline state to the paracrystalline state? Is native myelin paracrystalline? A study of the X-ray diffraction results from native myelin can answer this question. Paracrystalline materials exhibit certain characteristic X-ray diffraction effects.

III CONCLUSIONS OBTAINED FROM EXISTING X-RAY DATA

A Intensity decline

The lattice peak function for a one-dimensional paracrystal is $z(x) = H_0 + H_1 + H_{-1} + H_2 + H_{-2} + \cdots + H_m + H_{-m}$. The Fourier transform of $z(x)$, called the interference function $Z(X)$, is analogous to the reciprocal lattice of a crystal. The Fourier transform of $z(x)$ as a whole is a geometric progression of transforms of the H_j terms which allows a simplification of the equation: thus[11]

$$Z(X) = \frac{1 - |F|^2}{1 - 2|F|\cos(2\pi X) + |F|^2}$$

where $|F|$ is the even (cosine) Fourier transform of H_1. Since $H_1(x + d)$ is a gaussian curve, its Fourier transform is also a gaussian curve;

$$|F| = e^{-2\pi^2 X^2 s^2} \approx 1 - 2\pi^2 h^2 s^2/d^2 \quad \text{and} \quad hs/d \approx \sqrt{(1 - |F|)/19.7}.$$

As in a crystal the maxima occur at $X = h/d = hd^*$; h is an integer (the order of the reflection). Unlike a crystal the peak values for $Z(hd^*)$ decrease for increasing h, while the minimum between contiguous maxima increase. It is convenient to define k as the ratio of the height of a maximum to the adjacent minimum depth. $k = Z(hd^*)/Z([h + \frac{1}{2}]d^*)$. Thus k measures the oscillation of $Z(X)$; k approaches unity asymptotically. For $X = hd^*$, $Z_{max} = (1 + |F|)/(1 - |F|)$. Furthermore, $Z_{min} \approx 1/Z_{max}$; hence

$$k = \left(\frac{1 + |F|}{1 - |F|}\right)^2$$

Because $Z(X)$ decreases as h increases, paracrystalline X-ray diffraction data are characterized by the early occurrence of a region in which the maxima do not exceed background by more than 20%. At this point $k = 1.2$ which implies $|F| = 0.05$ and $s \approx d/4h$.

The intensity of the small angle X-ray diffraction data from native myelin is very rapidly attenuated. Caspar and Kirschner,[9] being assiduously careful, were able to record up to 18 diffraction orders from rabbit sciatic myelin ($d = 180$ Å) using an evacuated camera. An examination of their Figure 1 shows that all reflections beyond the 5th order are very weak and rest upon a relatively high background; it appears that few, if any, exceed background by more than 20%. Using $s = d/4h$, the value of s is estimated to fall between 3 and 7.5 Å for $h's = 15$ and 6, respectively. This result is in good agreement with the electron microscopy study. It supports the hypothesis that native hydrated myelin is paracrystalline.

B Reflection profile

Another distinguishing characteristic of most paracrystalline material is an increase in line-width with increasing angle.[11] Caspar and Kirschner[9] reported that the line-widths for rabbit and frog sciatic and optic nerves increase with increasing angle. They suggest attributing the line broadening to imperfect alignment of the nerve fibers. Imperfect alignment usually results in tangential broadening. Furthermore, the low angle arc divergence resulting from use of a vertical slit aperture should decrease with increasing angle. Therefore, it appears possible that the observed line-broadening in native hydrated myelin results from a paracrystalline stacking. Unfortunately the available experimental data is too qualitative to be used to make a more definitive analysis.

IV THE PARACRYSTALLINE CHARACTERIZATION OF MYELIN

A General parameters

Paracrystalline myelin is characterized by at least four parameters: d, s, N, and σ, where N is the mean number of lamellae per fiber within a nerve bundle and σ is the statistical fluctuation parameter for the distribution of n values about their mean N. Any experiment which alters myelin can affect some or all of these parameters. Variation of these parameters will cause concomitant changes in peak locations, peak intensities and peak profiles in the X-ray diffraction data.

B Swelling and arc length

The wrapping of myelin around a nerve axon is approximately a section of an Archimedes spiral; $r = d\theta$. Because of the invariant amount of membrane components, the arc length of the myelin spiral must remain relatively invariant during swelling. Thus, a myelin spiral of fixed arc length having increased d by swelling must either (1) reduce the number of its wrappings, changing N; (2) form innumerable irregularities such as the Schmidt–Lanterman clefts, changing s; or (3) fragment, changing N and σ. A Schwann cell wrapped 40 times about an axon of 1 μ thickness having an initial lamellar repeat of $d = 170$ Å would be expected to show an estimated reduction to about 33 wrappings when swollen to $d = 300$ Å. Furthermore, swelling of the central axon would cause an additional decrease in the value of N.

Plates I and III in Finean and Burge[4] show electron micrographs that clearly demonstrate that, in their experiments, the lamellar layers become irregularly spaced upon swelling in hypotonic solution. Extensive disruption of the myelin sheath was evident. The low angle X-ray diffraction diagrams in their Plate II (Ref. 4) show increasing line broadening during the swelling of frog sciatic nerve in hypotonic solution.

V SUMMARY

Both electron microscopic and X-ray diffraction evidence suggest that myelin is paracrystalline.

Acknowledgements

I thank Dr. Marshall L. Rennels of the Anatomy Department of the University of Maryland School of Medicine for the use of Figure 1. Supported by NSF grant GB 43447 and NIH grant CA16773. Computer time for this project was supported in full by facilities of the Computer Science Center of the University of Maryland.

References

1. F. O. Schmitt, R. S. Bear, and G. L. Clark, *Radiology*, **25**, 131 (1935).
2. B. B. Geren, *Exp. Cell. Res.*, **7**, 558 (1954).
3. J. B. Finean, *Circulation*, **26**, 1151 (1962).
4. J. B. Finean and R. E. Burge, *J. Mol. Biol.*, **7**, 672 (1963).
5. R. E. Burge and J. C. Draper, *Lab. Invest.*, **14**, 978 (1965).
6. C. K. Akers and D. F. Parsons, *Biophys. J.*, **10**, 116 (1970).
7. D. Harker, *Biophys. J.*, **12**, 1285 (1972).
8. C. R. Worthington and T. J. McIntosh, *Biophys. J.*, **14**, 703 (1974).
9. D. L. D. Caspar and D. A. Kirschner, *Nat. New Biol.*, **231**, 46 (1971).
10. R. Hosemann and S. N. Bagchi, *Direct Analysis of Diffraction by Matter*, North-Holland, Amsterdam (1962)—out of print since 1970—see also R. Hosemann, *Die Makromolekulare Chemie, Suppl. 1*, 559 (1975).
11. B. K. Vainshtein, *Diffraction of X-rays by Chain Molecules*, Elsevier, Amsterdam, Chap. V (1966).